

Article type : Full length original research paper

The novel sodium channel modulator GS-458967 (GS967) is an effective treatment  
in a mouse model of *SCN8A* encephalopathy

Erin M. Baker<sup>a</sup>, Christopher H. Thompson<sup>a</sup>, Nicole A. Hawkins<sup>a</sup>, Jacy L. Wagnon<sup>b</sup>, Eric R.  
Wengert<sup>c</sup>, Manoj K. Patel<sup>c</sup>, Alfred L. George, Jr.<sup>a</sup>, Miriam H. Meisler<sup>b</sup>, Jennifer A. Kearney<sup>a\*</sup>

<sup>a</sup>Department of Pharmacology, Northwestern University Feinberg School of Medicine,  
Chicago, IL, 60611, USA

<sup>b</sup>Department of Human Genetics, University of Michigan, Ann Arbor, MI 48109-5618

<sup>c</sup>Department of Anesthesiology, University of Virginia Health System, Charlottesville, VA 22908

Running Title: Efficacy of GS967 in *Scn8a*<sup>N1768D/+</sup> mice

This is the author manuscript accepted for publication and has undergone full peer review but has not been through the copyediting, typesetting, pagination and proofreading process, which may lead to differences between this version and the [Version of Record](#). Please cite this article as [doi: 10.1111/EPI.14196](https://doi.org/10.1111/EPI.14196)

This article is protected by copyright. All rights reserved

\*Corresponding Author:

Jennifer A. Kearney, Ph.D.

320 E. Superior St., Searle 8-450

Chicago, IL 60611

Phone: 312-503-4894

E-mail: [jennifer.kearney@northwestern.edu](mailto:jennifer.kearney@northwestern.edu) (JAK)

**Keywords:** epilepsy; voltage-gated sodium channel; pharmacology; mouse model; epileptic encephalopathy

14 text pages; 4027 words; 37 references; 5 figures; 1 tables

2 Supplemental Figures; 1 Supplemental Table

## SUMMARY

### Objective

*De novo* mutations of *SCN8A*, encoding the voltage-gated sodium channel Nav1.6, have been associated with a severe infant-onset epileptic encephalopathy. Individuals with *SCN8A* encephalopathy have a mean age of seizure onset of 4-5 months, with multiple seizure types that are often refractory to treatment with available drugs. Anecdotal reports suggest that high-dose phenytoin is effective for some patients, but there are associated adverse effects and potential toxicity. Functional characterization of several *SCN8A* encephalopathy variants has shown that elevated persistent sodium current is one of several common biophysical defects. Therefore, specifically targeting elevated persistent current may be a useful therapeutic strategy in some cases.

### Methods

The novel sodium channel modulator GS967 has greater preference for persistent versus peak current and nearly ten-fold greater potency than phenytoin. We evaluated the therapeutic effect of GS967 in the *Scn8a*-N1768D/+ mouse model carrying an *SCN8A* patient mutation that results in elevated persistent sodium current. We also performed patch clamp recordings to assess the effect of GS967 on peak and persistent sodium current and excitability in hippocampal neurons from *Scn8a*-N1768D/+ mice.

## Results

GS967 potently blocked persistent sodium current without affecting peak current, normalized action potential morphology, and attenuated excitability in neurons from heterozygous *Scn8a*-N1768D/+ mice. Acute treatment with GS967 provided dose-dependent protection against MES-induced seizures in *Scn8a*-N1768D/+ and wild-type mice. Chronic treatment of *Scn8a*-N1768D/+ mice with GS967 resulted in lower seizure burden and complete protection from seizure-associated lethality observed in untreated *Scn8a*-N1768D/+ mice. Protection was achieved at a chronic dose that did not cause overt behavioral toxicity or sedation.

## Significance

Persistent sodium current modulators like GS967 may be an effective precision targeting strategy for *SCN8A* encephalopathy and other functionally similar channelopathies when elevated persistent sodium current is the primary dysfunction.

**Keywords:** epilepsy; voltage-gated sodium channel; pharmacology; mouse model; epileptic encephalopathy

## Key Points

- GS967 potently suppressed persistent sodium current in acutely dissociated neurons and hyperexcitability in slices from heterozygous *Scn8a*-N1768D/+ mice
- Acute treatment with GS967 dose-dependently protected both *Scn8a*-N1768D/+ and wild-type mice against MES-induced seizures
- Chronic GS967 treatment was associated with significantly lower spontaneous seizure burden and completely protected *Scn8a*-N1768D/+ mice from seizure-associated lethality
- Chronic GS967 did not cause overt behavioral toxicity or sedation in wild-type mice at the effective anticonvulsant dose

## INTRODUCTION

Epilepsy is a common neurological disorder with a lifetime incidence of 1 in 26<sup>1</sup>. Mutations in genes encoding neuronal voltage-gated sodium channels have been implicated in several types of human epilepsy, including epileptic encephalopathies<sup>2</sup>. These are severe epilepsies with co-occurring cognitive, behavioral, and neurological deficits due to the combined effect of seizure

activity and the underlying mutation<sup>3</sup>. In recent years, over 150 cases of epileptic encephalopathy have been associated with *de novo* mutations in *SCN8A*, encoding the Nav1.6 voltage-gated sodium channel pore-forming (alpha) subunit. The clinical phenotype begins in the first year of life with pleiomorphic seizures that are difficult to control, delayed cognitive development and motor impairment<sup>4</sup>. *SCN8A* encephalopathy is also associated with an elevated risk for sudden unexpected death in epilepsy (SUDEP), making seizure control a high priority<sup>5;6</sup>.

The first report of *SCN8A* encephalopathy described a female proband with multiple seizure types, intellectual disability, developmental delay, and motor impairment<sup>2</sup>. She succumbed to SUDEP at 15 years of age. Whole genome sequencing of the family quartet identified the heterozygous, *de novo* mutation *SCN8A* p.Asn1768Asp (N1768D)<sup>7</sup>. Electrophysiological recording of sodium currents in ND7/23 cells expressing the mutant channel revealed a large persistent sodium current as the primary biophysical defect, as well as incomplete channel inactivation and a shift in the voltage dependence of steady-state fast inactivation<sup>7</sup>. Introduction of the N1768D mutation into the murine *Scn8a* gene resulted in a mouse model that recapitulates many features of the human syndrome<sup>8;9</sup>. Specifically, heterozygous *Scn8a*<sup>N1768D/+</sup> (*Scn8a*<sup>D/+</sup>) mice exhibit spontaneous seizures, ataxia, cardiac arrhythmia, and premature death, although the age of seizure onset at 2-4 months of age is late relative to the *SCN8A*-N1768D proband. Homozygous *Scn8a*<sup>N1768D/N1768D</sup> (*Scn8a*<sup>D/D</sup>) mice exhibit these features with earlier onset and accelerated progression. Similar to recordings in heterologous expression systems, neurons from *Scn8a*<sup>D/+</sup> mice have elevated persistent current and higher spontaneous firing rate compared to wild-type (WT) neurons<sup>7;10</sup>. The mouse model enables preclinical evaluation of potential anti-convulsant treatments for *SCN8A* encephalopathy.

Several types of biophysical defects have been documented for variants associated with *SCN8A* encephalopathy. Targeting persistent sodium current, one of the common primary biophysical defects in this disorder, may provide an effective precision therapeutic approach. Reports have described patients achieving seizure control with carbamazepine, oxcarbazepine, valproic acid, and most notably, high-dose phenytoin<sup>11-16</sup>. Phenytoin is a state-dependent sodium channel blocker with a small preference (~10%) for persistent current over peak current<sup>17</sup>. However, high dose phenytoin has significant safety concerns due to saturable metabolism and risk for

phenytoin poisoning<sup>18-21</sup>. GS-458967 (GS967) is a novel sodium channel modulator specifically developed to inhibit persistent sodium current, with a 42-fold preference for persistent versus peak current inhibition<sup>22</sup>. Our previous studies demonstrated that acute application of GS967 to hippocampal neurons did not affect the current-voltage relationship or voltage dependence of activation, but induced a hyperpolarized shift of steady-state channel inactivation and slowed both recovery from fast inactivation and onset of slow inactivation<sup>23</sup>. GS967 has also been reported to have strong use-dependent block<sup>24</sup>.

GS967 was previously tested in the *Scn2a*<sup>Q54</sup> mouse model with epilepsy caused by elevated persistent sodium current in hippocampal neurons<sup>25</sup>. Acute application of GS967 to neurons isolated from untreated *Scn2a*<sup>Q54</sup> mice reduced persistent sodium current and spontaneous firing, while GS967 treatment of *Scn2a*<sup>Q54</sup> mice reduced seizure burden and improved survival. Considering the etiological similarities between *Scn2a*<sup>Q54</sup> and *Scn8a*<sup>D/+</sup> mice, we hypothesized that treatment with GS967 may have a therapeutic benefit in the *Scn8a*<sup>D/+</sup> and *Scn8a*<sup>D/D</sup> mice.

In the current study, we tested the effect of GS967 on persistent sodium current and action potential firing in neurons, as well as seizure susceptibility, spontaneous seizures and survival of *Scn8a*<sup>D/+</sup> mice. We report that GS967 suppresses persistent sodium current and excitability in neurons *ex vivo*, and protects against seizures and premature lethality *in vivo*, supporting targeting of persistent sodium current as a potential therapeutic strategy for this disorder.

## METHODS

### Mice

*Scn8a*<sup>em1Mm</sup> mice were generated using TALEN technology and previously characterized<sup>8;9</sup>. The line was made congenic by continuous backcrossing to C3HeB/FeJ wild-type (WT) mice (Stock # 000658, Jackson Laboratory, Bar Harbor, ME) for more than 10 generations. Mice were genotyped by PCR of tail biopsy DNA as previously described<sup>8</sup>. Heterozygous experimental mice were obtained by breeding *Scn8a*<sup>D/+</sup> males with C3HeB/FeJ females. Homozygous experimental mice were generated by breeding *Scn8a*<sup>D/+</sup> males with *Scn8a*<sup>D/+</sup> females. Mice were housed in Specific Pathogen Free barrier facility with a 14/10 hour light/dark cycle and access to food and water *ad libitum*. Animal studies were approved by the Northwestern

University and the University of Virginia Animal Care and Use Committees in accordance with the NIH Guide for the Care and Use of Animals. Principles outlined in the ARRIVE (Animal Research: Reporting of in vivo Experiments) and Basel declaration (including the 3R concept) were considered in experimental design. Both male and female mice were used in all experiments.

## **Drugs**

GS967 was provided by Gilead Sciences (Foster City, CA, USA) or purchased from Cayman Chemical (Ann Arbor, MI, USA). Phenytoin sodium solution was manufactured by West-Ward Pharmaceuticals (Eatontown, NJ) and obtained from Patterson Veterinary Supply (Greeley, CO). Phenytoin for electrophysiology experiments was obtained from Sigma Aldrich (St. Louis, MO). Drug solutions for electrophysiology experiments were prepared in DMSO. For acute administration to mice in MES experiments, GS967 was solubilized in vegetable oil, and phenytoin sodium solution was diluted with 0.5% methyl cellulose in water. Vehicle control mice were administered either vegetable oil or 0.5% methyl cellulose in water. For chronic administration studies, mice were fed Purina 5001 rodent chow compounded with GS967 (8 mg per kg of chow; Research Diets, New Brunswick, NJ)<sup>23;25</sup>. The estimated dose was 1.5 mg/kg/day based on average daily consumption of 190 grams of chow per kg of body weight (<http://www.researchdiets.com/resource-center-page/typical-food-intake>). Previous studies showed that chronic treatment with this dose resulted in GS967 plasma and brain concentrations of  $1.0 \pm 0.08 \mu\text{M}$  and  $1.7 \pm 0.1 \mu\text{M}$ , respectively<sup>23</sup>. Chronic treatment with GS967 at 1.5 mg/kg/day did not cause overt adverse neurobehavioral or sedating effects in WT C3HeB/FeJ at 5-7 weeks of treatment (Supplemental Fig. S1).

## **Isolated Neuron Preparation and Electrophysiology Recording**

Neurons were acutely isolated from untreated *Scn8a*<sup>D/+</sup> mice and WT littermates between 30 and 35 days of age. Hippocampal neurons were isolated as previously described<sup>25</sup>. Whole-cell voltage clamp experiments of acutely isolated pyramidal neurons were performed at room temperature using previously described methods<sup>26;27</sup>. External recording solution contained (in mM): 20 NaCl, 100 N-methyl-D-glucamine, 10 HEPES, 1.8 CaCl<sub>2</sub>·2H<sub>2</sub>O, 2 MgCl<sub>2</sub>·6H<sub>2</sub>O, and 20 tetraethylammonium chloride with pH adjusted to 7.35 with HCl and osmolarity adjusted to

310 mOsmol/kg with sucrose. Internal solution consisted of (in mM): 5 NaF, 105 CsF, 20 CsCl, 2 EGTA, and 10 HEPES with pH adjusted to 7.35 with CsOH and osmolarity adjusted to 280 mOsmol/kg with sucrose. All whole-cell voltage clamp recordings utilized a holding potential of -120 mV. Voltage gated sodium currents were recorded in the absence and presence of 500 nM TTX, and analyzed following offline digital subtraction, as previously described<sup>26; 27</sup>. Persistent current was measured utilizing a 200 ms depolarizing step. Mean current in the final 10 ms was normalized to peak transient current. Statistical comparisons were made using Student's t-test or one-way ANOVA followed by Tukey's post hoc and  $p < 0.05$  was considered statistically significant.

### **Brain Slice Preparation and Electrophysiology Recording**

Brain slices were prepared from WT and *Scn8a*<sup>D/+</sup> mice (> 8 weeks of age) using a Leica VT1200 vibratome as previously described<sup>10</sup>. CA1 pyramidal neurons were visually identified using infrared video microscopy (Hamamatsu) with a Zeiss Axioscope microscope. Whole-cell current-clamp recordings were performed as previously described<sup>10</sup>. During recordings, slices were held in a small chamber and superfused with oxygenated ACSF (in mM: 125 NaCl, 2.5 KCl, 1.25 NaH<sub>2</sub>PO<sub>4</sub>, 2 CaCl<sub>2</sub>, 1 MgCl<sub>2</sub>, 0.5 L-ascorbic acid, 10 glucose, 25 NaHCO<sub>3</sub>, and 2 sodium pyruvate (osmolarity 300-312 mOsm/L) at ~28°C at a rate of 1-2 mL/min. Intracellular recording solution containing (in mM): 120 K-gluconate, 10 NaCl, 2 MgCl<sub>2</sub>, 0.5 K<sub>2</sub>EGTA, 10 HEPES, 4 Na<sub>2</sub>ATP, 0.3 NaGTP, and pH was adjusted to 7.2 with KOH (osmolarity 270-290 mOsmol/L)

Action potentials (APs) were evoked using a depolarizing current injection step of 400 pA. To standardize across neurons, resting membrane potentials were maintained at -70 mV by injection of DC current. Only depolarizing events that consisted of a single observable peak initiating from threshold and had an upstroke velocity >150 mV/ms were considered as APs. Early after-depolarizing events (EADs) were identified as spikelets that occurred during the repolarizing phases of the initial AP and had slower upstroke velocities (>15 mV/ms), longer widths and depolarized thresholds. Input resistance was calculated using a -20 pA hyperpolarizing current injection step. The approximate rheobase for each cell was defined as the highest current injection step that did not evoke any APs. AP duration (APD) was defined as the width of the AP at the half way voltage between threshold and AP peak and was measured for the first AP

elicited during a 400 pA current injection. In order to measure intrinsic membrane and AP properties, a ramp of depolarizing current (0-400 pA) was injected into each neuron over a 4 sec time period. Threshold was identified as the membrane potential at which the upstroke velocity was 5% of its maximum<sup>28</sup>. AP amplitude, upstroke velocity and downstroke velocity were calculated using the first evoked AP during the current ramp. Amplitude was defined as the difference between threshold and AP peak, while upstroke velocity and downstroke velocity were defined as the maximum and minimum slope of the evoked AP, respectively.

### **Maximal Electroshock**

At 4 weeks of age, mice were assigned to treatment groups by block randomization and received an intraperitoneal injection of test compound (PHT or GS967) or their respective vehicle in a volume of 10 ml/kg body weight two hours prior to testing. Maximal electroshock (MES) tests were conducted at the previously determined time-to-peak effect for GS967 and phenytoin<sup>25</sup>. Corneal electroshock was delivered using a pulse generator set at a frequency of 60 Hz and 0.5 ms pulse width (Ugo Basile) with shock duration 0.2 s and current 20 mA (120 mC) for *Scn8a*<sup>D/+</sup> and 0.4 s, and 60 mA (720 mC) for WT mice. Mice were scored for the presence or absence of full tonic hindlimb extension (hindlimbs at a 180° angle to torso) occurring within 5 seconds of the shock. EC<sub>50</sub> values were determined from dose-response curves generated and compared with GraphPad Prism software.

### **Survival**

At 6 weeks of age, heterozygous *Scn8a*<sup>D/+</sup> mice were assigned to either GS967 or control treatment groups by block randomization. Mice in the GS967 treatment group were provided chow containing GS967 (8 mg per kg of chow; Research Diets, New Brunswick, NJ). The estimated dose was 1.5 mg/kg/day based on average consumption of 4 grams of chow per day. Previous studies established that this dose results in plasma levels of ~1 μM<sup>23;25</sup>. Survival was monitored up to 9 months of age by performing census checks 3-4 days per week. Homozygous *Scn8a*<sup>D/D</sup> mice were generated by crossing *Scn8a*<sup>D/+</sup> males and *Scn8a*<sup>D/+</sup> females. When the resulting offspring were 5 days of age, the lactating dam was either maintained on control chow or switched to GS967 chow. Previous studies showed that GS967 passes freely to



nursing pups resulting a plasma concentration of  $\sim 1 \mu\text{M}^{23}$ . Survival of the *Scn8a*<sup>D/D</sup> pups was monitored by performing census checks 6-7 days per week.

Survival was assessed with Kaplan-Meier analysis and compared between groups using the Mantel Cox Log Rank test with  $p < 0.05$  considered statistically significant.

### **Video-Electroencephalography (EEG)**

At 6 weeks of age, *Scn8a*<sup>D/+</sup> mice and WT littermates were assigned to either GS967 or control treatment groups by block randomization. At age 70-80 days, mice were anesthetized with isoflurane and fitted with a pre-fabricated headmount (Pinnacle Technology). Following at least 48 hours of recovery, mice underwent continuous video-EEG recording for 5-13 days.

Additional days of continuous video-only recording were obtained (range 3-26 days). Digitized EEG data was acquired and analyzed with Sirenia software (Pinnacle Technology). Epileptiform activity was scored offline by a blinded observer to identify electrographic seizures and behavioral correlates. The behavioral component of seizures scored by video-only were indistinguishable from those scored by epileptiform activity. Seizure frequencies were calculated for each individual animal and compared between treated and untreated *Scn8a*<sup>D/+</sup> mice using a Mann-Whitney test with  $p < 0.05$  considered statistically significant.

### **CNS Safety Screen**

At 6 weeks of age, WT C3HeB/FeJ mice were assigned to either GS967 or control treatment groups by block randomization and commenced treatment. At 11-13 weeks of age, mice were tested on three assays on consecutive days using a modified Irwin screen (day 1)<sup>29</sup>, open field test (day 2) and rotarod test (day 3). All testing was conducted between 9:00am and 1:00pm. For the open field assay, mice were placed in a new environment and tracked for 10 minutes (Limelight software, Actimetrics). Mice were scored on total distance traveled. For the rotarod assay, mice underwent a training trial (4 rpm) and then three test trials with acceleration from 4-40 rpm (Panlab/Harvard Apparatus). Trials were separated by 15 minutes of rest. Latency to fall was recorded for the three trials and averaged. Parametric data were compared using Student's t-tests and non-parametric data were compared using Mann-Whitney U-test, with  $p < 0.05$  was considered statistically significant. No significant sex differences were observed, so groups were collapsed across sex.

## RESULTS

### **GS967 suppresses persistent current in hippocampal neurons from *Scn8a*<sup>D/+</sup> mice**

Using whole-cell voltage clamp recording, we measured persistent sodium current in acutely isolated hippocampal pyramidal neurons from postnatal day 30 to 35 (P30-P35) *Scn8a*<sup>D/+</sup> mice. Persistent current was assessed as tetrodotoxin-sensitive current following a 200 ms depolarization. In untreated neurons from *Scn8a*<sup>D/+</sup> mice, persistent current was equal to  $1.7 \pm 0.3$  % of peak current ( $n = 8$ ) (Fig. 1A, black trace). The magnitude of persistent current is lower than previous reports due to differences in cell type and recording conditions<sup>10</sup>. To assess the ability of either GS967 or phenytoin to selectively inhibit persistent sodium current, neurons were acutely treated with drug concentrations approximating the therapeutic free drug concentration in mouse brain, 200 nM GS967 or 4  $\mu$ M phenytoin. In the presence of GS967, persistent current was more than ten-fold lower than in the absence of compound ( $0.12 \pm 0.06$ % of peak current,  $n = 7$ ;  $p < 0.001$ , one-way ANOVA and Tukey's post hoc). In the presence of phenytoin, persistent current was approximately two-fold lower than drug-free conditions ( $0.94 \pm 0.09$ % of peak current,  $n=6$ ;  $p < 0.04$ ). Thus, GS967 was more potent than phenytoin in suppressing persistent current mediated by the mutant channel ( $p < 0.04$ ) (Fig. 1A-B). Importantly, neither compound significantly altered peak sodium current under these conditions (Fig. 1C).

### **GS967 suppresses early afterdepolarizations (EADs) and reduces neuronal excitability in CA1 pyramidal neurons from *Scn8a*<sup>D/+</sup> mice**

AP waveforms from *Scn8a*<sup>D/+</sup> mice CA1 pyramidal neurons exhibited prominent EADs that were evident during the repolarization phase of APs (Fig. 2A-C), in agreement with previous studies<sup>30</sup>. These abnormal waveforms were not observed in WT controls (Fig. 2D). Addition of GS967 had a profound effect on EADs, reducing their number by 41% at 500 nM and 50% at 1  $\mu$ M GS967 (Fig 2B-C). GS967 had no effect on AP firing frequencies from either *Scn8a*<sup>D/+</sup> or WT (+/+) neurons (Fig 2Ai-Di). Analysis of AP parameters revealed differences between *Scn8a*<sup>D/+</sup> and WT neurons (Table S1). GS967 (1  $\mu$ M) decreased AP amplitude and upstroke velocity in both *Scn8a*<sup>D/+</sup> and WT neurons. AP thresholds were also depolarized in *Scn8a*<sup>D/+</sup> neurons, but

not WT (Fig 2E, Table S1). APDs were not changed (Table S1). These findings demonstrate that GS967 can modulate intrinsic hyper-excitability of CA1 neurons from *Scn8a*<sup>D/+</sup> mice.

### **GS967 is more potent than phenytoin for seizure protection in the MES assay**

We assessed acute anticonvulsant activity of GS967 and phenytoin using the maximal electroshock (MES) paradigm in *Scn8a*<sup>D/+</sup> mice and WT littermates. The electroconvulsive stimulus (ECS) required to induce maximal hindlimb extension in >95% of mice (ECS<sub>95</sub>) was determined for both genotypes. *Scn8a*<sup>D/+</sup> mice required a stimulus of 120 mC compared to 720 mC for WT mice. Varying doses of GS967 or phenytoin were administered two hours prior to MES induction using the genotype-appropriate ECS<sub>95</sub>. Both GS967 and phenytoin provided dose-dependent protection against MES-induced tonic hindlimb seizures, with GS967 exhibiting greater potency. *Scn8a*<sup>D/+</sup> mice were protected from maximal hindlimb extension with a calculated EC<sub>50</sub> of 1.2 ± 0.2 mg/kg for GS967 and 5.3 ± 0.7 mg/kg for phenytoin (Fig. 3A). Similar results were found in WT mice with an EC<sub>50</sub> of 0.7 ± 0.2 mg/kg for GS967 and 6.9 ± 0.5 mg/kg for phenytoin (Fig. 3B).

### **Chronic GS967 treatment prolongs survival of *Scn8a*<sup>D/+</sup> mice**

Survival of *Scn8a*<sup>D/+</sup> mice is limited, with fewer than 50% of mice surviving to 6 months of age<sup>9</sup>. To determine whether chronic treatment with GS967 would extend survival, *Scn8a*<sup>D/+</sup> mice were fed chow containing GS967 (estimated dose 1.5 mg/kg/day) beginning at 6 weeks and continuing until 6 months of age. This dose was previously shown to be anticonvulsant in *Scn2a*<sup>Q54</sup> and *Scn1a*<sup>+/-</sup> mouse models<sup>23;25</sup> and does not produce any signs of behavioral toxicity or sedation (Supplementary Fig. S1). Treatment with GS967 beginning at 6 weeks and continuing to 6 months of age completely rescued premature lethality of *Scn8a*<sup>D/+</sup> mice, with 100% of GS967-treated mice (n = 32) surviving to 6 months of age, compared with only 24% of untreated mice (7/29) (p < 0.001, LogRank Mantel-Cox). Removal of the GS967 chow at 6 months of age resulted in rapid loss of protection and 65% of the previously treated mice died within the following 3 months (Fig. 4A). Loss of GS967 benefit following withdrawal suggests that it acts primarily as an anticonvulsant rather than a disease-modifying treatment.

The phenotype of homozygous *Scn8a*<sup>D/D</sup> mice is much more severe than heterozygous *Scn8a*<sup>D/+</sup> mice or heterozygous patients. *Scn8a*<sup>D/D</sup> mice exhibit 100% lethality by 21 days of age<sup>9</sup>.

Treatment of *Scn8a*<sup>D/D</sup> mice, achieved by feeding nursing dams GS967 beginning at P5, extended survival by one week ( $p < 0.001$ , LogRank Mantel-Cox) (Fig. 4B).

### **GS967 reduces spontaneous seizures in *Scn8a*<sup>D/+</sup> mice**

Previous reports showed that *Scn8a*<sup>D/+</sup> mice have spontaneous seizures with onset at 2 to 4 months of age, followed by death within a few days of seizure onset<sup>9;31</sup>. To evaluate the effect of GS967 on spontaneous seizures, mice were continuously observed with a combination of video-electroencephalography (EEG) monitoring and continuous video monitoring for several hundred hours (Fig. 5; Supplemental Figure S2). Only 2/7 GS treated mice experienced any seizures during the time of monitoring, compared with 7/7 untreated mice (Table 1). All recorded seizures in *Scn8a*<sup>D/+</sup> mice initiated with a tonic phase and culminated in full tonic hindlimb extension, with the angle of hindlimbs to the torso  $\geq 180^\circ$ . Several of the untreated mice exhibited seizure clustering, with days of seizure freedom separating periods of high seizure frequency (Supplemental Figure S2). Untreated *Scn8a*<sup>D/+</sup> mice also exhibited seizures with multiple tonic to tonic-clonic transitions. In contrast, seizures in the GS967-treated *Scn8a*<sup>D/+</sup> mice had a single tonic phase that terminated with post-ictal suppression. Combined analysis of video-EEG and video monitoring showed that *Scn8a*<sup>D/+</sup> mice treated with GS967 had significantly lower seizure frequency, with  $0.3 \pm 0.2$  seizures/24-hours in GS967-treated compared with  $1.6 \pm 0.4$  seizures/24-hours in untreated mice ( $p < 0.004$ , Fig. 5C, Table 1). No seizures were observed in WT littermate mice (Table 1). These data demonstrate that GS967 has a potent anti-seizure effect in a mouse model of *SCN8A* encephalopathy.

## **DISCUSSION**

In this study, we demonstrated that GS967 provided significant reduction in spontaneous seizure burden and improved survival in the *Scn8a*<sup>D/+</sup> epilepsy model. We also demonstrated that GS967 provided protection from acute MES-induced seizures in both *Scn8a*<sup>D/+</sup> and WT mice.

*GS967 is a potent blocker of persistent current arising from the Scn8a-N1768D mutation*

We and others previously reported that GS967 is a potent inhibitor of persistent sodium current<sup>22; 24; 32-34</sup>, with 9-fold greater potency than phenytoin in hippocampal pyramidal neurons from *Scn2a*<sup>Q54</sup> mice<sup>25</sup>. Consistent with these reports, acute application of 200 nM GS967 or 4  $\mu$ M

phenytoin to acutely dissociated hippocampal neurons isolated from *Scn8a<sup>D/+</sup>* mice resulted in inhibition of persistent sodium current without significantly affecting peak current. Consistent with this, acute application of GS967 to hippocampal slices from *Scn8a<sup>D/+</sup>* mice resulted in normalization of intrinsic excitability in CA1 neurons.

#### *Anticonvulsant activity of GS967*

To assess anticonvulsant activity of GS967, we first established the dose-response relationship of acutely administered GS967 for MES-induced seizures, using the conventional anticonvulsant phenytoin as a comparator. We demonstrated that GS967 provided dose-dependent protection against MES-induced seizures with ~5-10-fold greater potency than phenytoin in both WT and *Scn8a<sup>D/+</sup>* mice. Chronic administration of GS967 was associated with a dramatically lower spontaneous seizure frequency and prevented lethality at a dose that did not cause overt neurobehavioral toxicity or sedation. GS967 treatment provided complete protection in heterozygous *Scn8a<sup>D/+</sup>* mice that have the same genotype as the N1768D proband with *SCN8A* encephalopathy, resulting from a heterozygous *de novo* mutation. Even in the severely affected homozygous *Scn8a<sup>D/D</sup>* mice, GS967 extended survival from 3 weeks to 4 weeks of age. Similar to individuals with *SCN8A* encephalopathy, *Scn8a<sup>D/+</sup>* mice exhibit tonic and/or tonic-clonic seizures that may occur in clusters. Video-EEG monitoring showed that untreated *Scn8a<sup>D/+</sup>* mice often exhibit prolonged seizures with multiple tonic to tonic-clonic transitions. GS967-treated mice were completely protected from these multi-phase events and exhibited only isolated seizures with a single tonic phase. These observations suggest that GS967 may reduce the extent of ictal events, in addition to reducing seizure frequency. These effects are likely to contribute to the survival benefit, because poor seizure control and frequent, prolonged generalized tonic-clonic seizures are major risk factors for SUDEP<sup>35</sup>. GS967 was originally developed as an antiarrhythmic compound<sup>22; 24; 32; 33</sup>, and may also have a direct effect on the heart. This effect may contribute to the protection against sudden death, since *Scn8a<sup>D/+</sup>* mice have hyperexcitable cardiomyocytes and episodes of bradycardia observed in electrocardiograms<sup>36</sup>.

Although we demonstrate dramatic improvement in seizure burden and survival in *Scn8a<sup>D/+</sup>* mice treated with GS967, there are some limitations of our preclinical study that warrant consideration. First, GS967 treatment was commenced prior to seizure onset and it is not known if commencing treatment after fulminant onset would provide the same level of protection.

Second, the age of seizure onset in the mouse *Scn8a*<sup>D/+</sup> model is later than that observed in the proband, suggesting that the mouse model does not directly phenocopy the human case. Third, *SCN8A* encephalopathy includes mutations that result in a variety of Nav1.6 dysfunction ranging from gain-of-function defects, including but not limited to persistent sodium current, to loss-of-function defects. This suggests that GS967 would not necessarily be broadly effective in all cases of *SCN8A* encephalopathy, but rather that knowledge of the specific channel dysfunction may provide additional information for rational therapy choice.

Beyond *Scn8a*<sup>D/+</sup> mice, GS967 was previously shown to reduce seizure burden and improve survival in *Scn2a*<sup>Q54</sup> mice, which share the biophysical defect of elevated persistent sodium current<sup>25,37</sup>. GS967 was also shown to have a protective effect in the *Scn1a*<sup>+/-</sup> Dravet mouse model that has reduced activity in inhibitory neurons and elevated excitability in excitatory neurons mice<sup>23,26</sup>. However, there is no evidence for alteration of persistent current in this model, suggesting that GS967 can have protective benefit in a genetic model with an alternate underlying mechanism. Furthermore, we demonstrated here and in a previous report that GS967 has potent anti-seizure activity in the MES assay in WT mice<sup>25</sup>, supporting potentially broader applicability of GS967 in epilepsies with divergent etiologies.

### Conclusions

We demonstrate that targeting of a specific biophysical defect in Nav1.6 gating observed with some *SCN8A* patient mutations is an effective antiepileptic treatment strategy in *Scn8a*<sup>D/+</sup> mice. This supports a precision medicine approach to *SCN8A* encephalopathy, and suggests that defining the biophysical defect may provide valuable information to guide therapy. Moreover, results from acute MES studies and other genetic models, suggest that suppression of Nav1.6 activity may also be a general therapeutic approach relevant to other genetic and non-genetic epilepsies.

### ACKNOWLEDGMENTS

We thank Nicole Zachwieja and Tatiana Abramova for technical assistance, and Lyndsey Anderson for experimental guidance. Supported by Northwestern University Feinberg School of Medicine and NIH grant R01 NS103090 (MKP). E.M.B. is supported by a predoctoral

fellowship from the PhRMA foundation. Initial aliquots of GS967 were provided Gilead Sciences.

## **DISCLOSURE OF CONFLICTS OF INTEREST**

Authors JAK and ALG have received support from, and/or have served as a paid consultant for Praxis Precision Medicines. ALG served as a paid consultant for Gilead Sciences. The remaining authors have no conflicts of interest.

## **ETHICAL PUBLICATION STATEMENT**

We confirm that we have read the Journal's position on issues involved in ethical publication and affirm that this report is consistent with those guidelines.

## **REFERENCES**

1. Hesdorffer DC, Logroscino G, Benn EK, et al. Estimating risk for developing epilepsy: a population-based study in Rochester, Minnesota. *Neurology* 2011;76:23-27.
2. Meisler MH, Kearney JA. Sodium channel mutations in epilepsy and other neurological disorders. *J Clin Invest* 2005;115:2010-2017.
3. Scheffer IE, Berkovic S, Capovilla G, et al. ILAE classification of the epilepsies: Position paper of the ILAE Commission for Classification and Terminology. *Epilepsia* 2017;58:512-521.
4. Hammer MF, Wagnon JL, Mefford HC, et al. SCN8A-Related Epilepsy with Encephalopathy. In Pagon RA, Adam MP, Ardinger HH, et al. (Eds) GeneReviews(R), University of Washington, Seattle: Seattle (WA); 2016.
5. Wagnon JL, Meisler MH. Recurrent and Non-Recurrent Mutations of SCN8A in Epileptic Encephalopathy. *Front Neurol* 2015;6:104.
6. Harden C, Tomson T, Gloss D, et al. Practice guideline summary: Sudden unexpected death in epilepsy incidence rates and risk factors: Report of the Guideline Development, Dissemination, and Implementation Subcommittee of the American Academy of Neurology and the American Epilepsy Society. *Neurology* 2017;88:1674-1680.

7. Veeramah KR, O'Brien JE, Meisler MH, et al. De novo pathogenic SCN8A mutation identified by whole-genome sequencing of a family quartet affected by infantile epileptic encephalopathy and SUDEP. *Am J Hum Genet* 2012;90:502-510.
8. Jones JM, Meisler MH. Modeling Human Epilepsy by TALEN Targeting of Mouse Sodium Channel Scn8a. *Genesis* 2014;52:141-148.
9. Wagnon JL, Korn MJ, Parent R, et al. Convulsive seizures and SUDEP in a mouse model of SCN8A epileptic encephalopathy. *Hum Mol Genet* 2015;24:506-515.
10. Ottolini M, Barker BS, Gaykema RP, et al. Aberrant Sodium Channel Currents and Hyperexcitability of Medial Entorhinal Cortex Neurons in a Mouse Model of SCN8A Encephalopathy. *J Neurosci* 2017;37:7643-7655.
11. Barker BS, Ottolini M, Wagnon JL, et al. The SCN8A encephalopathy mutation p.Ile1327Val displays elevated sensitivity to the anticonvulsant phenytoin. *Epilepsia* 2016;57:1458-1466.
12. Boerma RS, Braun KP, van den Broek MP, et al. Remarkable Phenytoin Sensitivity in 4 Children with SCN8A-related Epilepsy: A Molecular Neuropharmacological Approach. *Neurotherapeutics* 2016;13:192-197.
13. Braakman HM, Verhoeven JS, Erasmus CE, et al. Phenytoin as a last-resort treatment in SCN8A encephalopathy. *Epilepsia Open* 2017;2:343-344.
14. Larsen J, Carvill GL, Gardella E, et al. The phenotypic spectrum of SCN8A encephalopathy. *Neurology* 2015;84:480-489.
15. Meisler MH, Helman G, Hammer MF, et al. SCN8A encephalopathy: Research progress and prospects. *Epilepsia* 2016;57:1027-1035.
16. Wang J, Gao H, Bao X, et al. SCN8A mutations in Chinese patients with early onset epileptic encephalopathy and benign infantile seizures. *BMC Med Genet* 2017;18:104.
17. Segal MM, Douglas AF. Late sodium channel openings underlying epileptiform activity are preferentially diminished by the anticonvulsant phenytoin. *J Neurophysiol* 1997;77:3021-3034.
18. Imam SH, Landry K, Kaul V, et al. Free phenytoin toxicity. *Am J Emerg Med* 2014;32:1301 e1303-1304.
19. Marin LL, Garcia-Penas JJ, Herguedas JL, et al. Phenytoin-induced visual disturbances mimicking Delirium Tremens in a child. *Eur J Paediatr Neurol* 2010;14:460-463.
20. Phelps SJ, Baldree LA, Boucher BA, et al. Neuropsychiatric toxicity of phenytoin. Importance of monitoring phenytoin levels. *Clin Pediatr (Phila)* 1993;32:107-110.



21. Robertson K, von Stempel CB, Arnold I. When less is more: a case of phenytoin toxicity. *BMJ Case Rep* 2013;2013.
22. Belardinelli L, Liu G, Smith-Maxwell C, et al. A novel, potent, and selective inhibitor of cardiac late sodium current suppresses experimental arrhythmias. *J Pharmacol Exp Ther* 2013;344:23-32.
23. Anderson LL, Hawkins NA, Thompson CH, et al. Unexpected Efficacy of a Novel Sodium Channel Modulator in Dravet Syndrome. *Sci Rep* 2017;7:1682.
24. Potet F, Vanoye CG, George AL, Jr. Use-Dependent Block of Human Cardiac Sodium Channels by GS967. *Mol Pharmacol* 2016;90:52-60.
25. Anderson LL, Thompson CH, Hawkins NA, et al. Antiepileptic activity of preferential inhibitors of persistent sodium current. *Epilepsia* 2014;55:1274-1283.
26. Mistry AM, Thompson CH, Miller AR, et al. Strain- and age-dependent hippocampal neuron sodium currents correlate with epilepsy severity in Dravet syndrome mice. *Neurobiology of Disease* 2014;65:1-11.
27. Thompson CH, Hawkins NA, Kearney JA, et al. CaMKII modulates sodium current in neurons from epileptic Scn2a mutant mice. *Proc Natl Acad Sci U S A* 2017;114:1696-1701.
28. Yamada-Hanff J, Bean BP. Persistent sodium current drives conditional pacemaking in CA1 pyramidal neurons under muscarinic stimulation. *J Neurosci* 2013;33:15011-15021.
29. Irwin S. Comprehensive observational assessment: Ia. A systematic, quantitative procedure for assessing the behavioral and physiologic state of the mouse. *Psychopharmacologia* 1968;13:222-257.
30. Lopez-Santiago LF, Yuan Y, Wagnon JL, et al. Neuronal hyperexcitability in a mouse model of SCN8A epileptic encephalopathy. *Proceedings of the National Academy of Sciences* 2017;114:2383-2388.
31. Sprissler RS, Wagnon JL, Bunton-Stasyshyn RK, et al. Altered gene expression profile in a mouse model of SCN8A encephalopathy. *Exp Neurol* 2017;288:134-141.
32. Pezhouman A, Madahian S, Stepanyan H, et al. Selective inhibition of late sodium current suppresses ventricular tachycardia and fibrillation in intact rat hearts. *Heart Rhythm* 2014;11:492-501.
33. Sicouri S, Belardinelli L, Antzelevitch C. Antiarrhythmic effects of the highly selective late sodium channel current blocker GS-458967. *Heart Rhythm* 2013;10:1036-1043.
34. Hirakawa R, El-Bizri N, Shryock JC, et al. Block of Na<sup>+</sup> currents and suppression of action potentials in embryonic rat dorsal root ganglion neurons by ranolazine. *Neuropharmacology* 2012;62:2251-2260.

35. Lhatoo S, Noebels J, Whittemore V, et al. Sudden unexpected death in epilepsy: Identifying risk and preventing mortality. *Epilepsia* 2015;56:1700-1706.
36. Frasier CR, Wagnon JL, Bao YO, et al. Cardiac arrhythmia in a mouse model of sodium channel SCN8A epileptic encephalopathy. *Proc Natl Acad Sci U S A* 2016.
37. Kearney JA, Plummer NW, Smith MR, et al. A gain-of-function mutation in the sodium channel gene *Scn2a* results in seizures and behavioral abnormalities. *Neuroscience* 2001;102:307-317.

## FIGURE LEGENDS

**Figure 1.** GS967 inhibits persistent sodium current in acutely isolated hippocampal pyramidal neurons from *Scn8a<sup>D/+</sup>* mice. A, Representative traces showing persistent sodium current of untreated (black), GS967 treated (red), and phenytoin (PHT) treated (blue) neurons from *Scn8a<sup>D/+</sup>* mice. B&C, Summary data of persistent sodium current (B) and current-voltage relationship for peak sodium current (C) for untreated (black symbols, n = 8), phenytoin treated (blue symbols, n = 6), and GS967 treated (red symbols, n = 7) neurons from *Scn8a<sup>D/+</sup>* mice. Open symbols represent individual cells, while closed symbols represent mean  $\pm$  S.E.M. Statistical comparison were performed using one-way ANOVA followed by Tukey's post-test. \* represent statistical difference compared to untreated cells for phenytoin (p < 0.04 and GS967 (p < 0.001) treated cells.

**Figure 2.** GS967 suppresses early afterdepolarizations and reduces intrinsic excitability of CA1 pyramidal neurons from *Scn8a<sup>D/+</sup>* mice. A-D, upper panel traces show representative APs evoked using a 400 pA depolarizing current injection step. Black, before GS967; red, after GS967 at (A) 200 nM (n = 8 from 3 mice), (B) 500 nM (n = 12 from 3 mice), and (C) 1  $\mu$ M (n = 13 from 7 mice). (D) WT (+/+), n = 11 from 3 mice. Lower panels, representative EADs and (Ai-Di) bar/scatter plots showing effect of GS967 on APs and EADs evoked by a current injection step of 400 pA. (E) Representative trace for slow current ramp recorded from a CA1 pyramidal neuron before (black) and after (red) GS967 at 500 nM. Values are mean  $\pm$  SEM. Significant results were determined using paired student's t-test with alpha set to 0.05.

**Figure 3.** GS967 protects against MES-induced seizures in *Scn8a<sup>D/+</sup>* and wild-type (WT) mice with greater potency than phenytoin (PHT). Mice were pre-treated with test compound or vehicle and then received an electroconvulsive stimulus determined to reliably elicit seizures with maximal hindlimb extension in *Scn8a<sup>D/+</sup>* (120 mC) or WT (720 mC) mice. A, Dose response curves of GS967 and phenytoin for MES seizures in *Scn8a<sup>D/+</sup>* mice. The curve for GS967 is significantly shifted compared to phenytoin and the estimated EC<sub>50</sub> for GS967 and phenytoin are  $1.1 \pm 0.23$  mg/kg and  $5.33 \pm 0.69$  mg/kg, respectively ( $p < 0.001$ ,  $n = 5-24$ , Student's t-test). Symbols represent mean  $\pm$  S.E.M. B, Dose response curves of GS967 and phenytoin for MES seizures in WT mice. The curve is also significantly shifted and the estimated EC<sub>50</sub> for GS967 and phenytoin are  $0.70 \pm 0.22$  mg/kg and  $6.93 \pm 0.45$  mg/kg, respectively ( $p < 0.001$ ,  $n = 6-26$ , Student's t-test).

**Figure 4.** Treatment with GS967 significantly prolongs survival in heterozygous and homozygous mutants. A, Kaplan-Meier survival curves comparing untreated and GS967-treated *Scn8a<sup>D/+</sup>* mice. Treatment was started at 6 weeks of age (first dashed line) and was withdrawn at 6 months (second dashed line). Survival was significantly different between treatment groups ( $p < 0.001$ ;  $n = 29-32$ ; Mantel Cox Log Rank test). B, Kaplan-Meier survival curves comparing untreated and GS967-treated *Scn8a<sup>D/D</sup>* mice. Treatment was started at 5 days of age (dashed line). Survival difference between treatment groups was significant ( $p < 0.001$ ;  $n=6-8$ ; Mantel Cox Log Rank test).

**Figure 5.** Treatment with GS967 reduces the spontaneous seizure frequency in *Scn8a<sup>D/+</sup>* mice. A, Schematic representation of timeline for treatment, surgery, and monitoring of mice. B, Representative EEG trace of an electrographic seizure in a *Scn8a<sup>D/+</sup>* mouse. Channel 1 indicates left anterior to right anterior, Channel 2 indicates right anterior to left posterior. C, Seizure frequency was significantly lower in *Scn8a<sup>D/+</sup>* mice treated with GS967 compared to untreated ( $p < 0.004$ ; Mann-Whitney test;  $n = 7$  per group). Symbols represent mean  $\pm$  S.E.M.

**Table 1.** Extended spontaneous seizure monitoring in *Scn8a<sup>D/+</sup>* and WT mice treated chronically with 1.5 mg/kg/day GS967 and untreated controls.

Treatment	Genotype	n	Total # of hours monitored	Avg # of hours monitored per animal $\pm$ SEM (range)	Total # of seizures	% of seizures with multiple transitions	Avg Seizure Frequency* (seizures per 24 hours $\pm$ SEM)	Fraction of mice with observed seizures
GS967	<i>Scn8a<sup>D/+</sup></i>	7	1699	243 $\pm$ 52 (62-361)	9	0 %	0.3 $\pm$ 0.2	2 / 7
Untreated	<i>Scn8a<sup>D/+</sup></i>	7	2189	313 $\pm$ 94 (68-614)	137	46 %	1.6 $\pm$ 0.4	7 / 7
GS967	WT	3	628	209 $\pm$ 172 (102-408)	0	0 %	0 $\pm$ 0.0	0 / 3
Untreated	WT	2	96	48 $\pm$ 24 (24-72)	0	0 %	0 $\pm$ 0.0	0 / 2

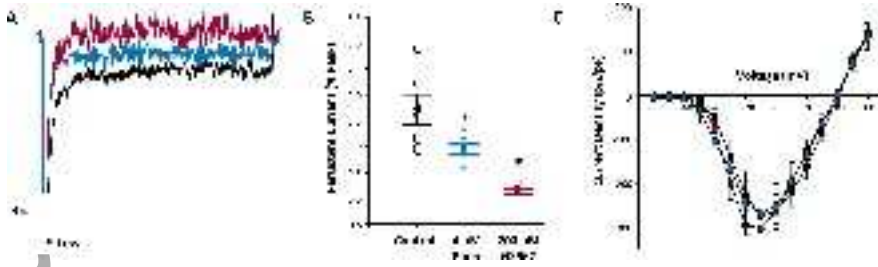
\*Calculated by averaging individual seizure frequencies within each group.

### Supplemental Information

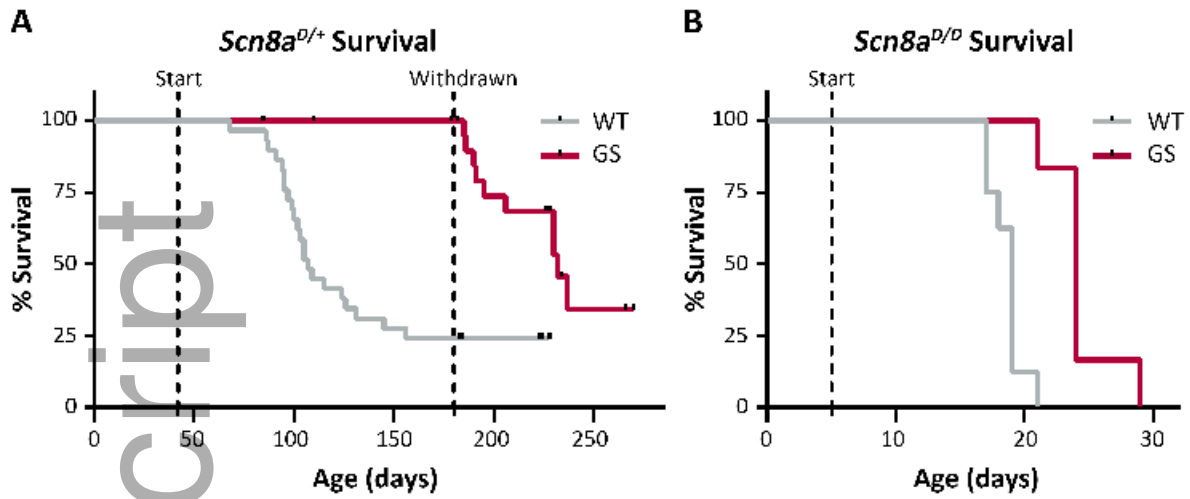
**Supplemental Figure S1.** Chronic treatment with GS967 for 5-7 weeks does not result in signs of neurobehavioral toxicity or sedation. At 6 weeks of age, WT C3HeB/FeJ mice were assigned to 1.5 mg/kg/day GS967 or control chow groups by block randomization. At 11-13 weeks of age, mice were tested in three assays on consecutive days. A, Modified Irwin screen conducted on day 1 showed no significant difference in neurobehavioral scores between GS967-treated and untreated control mice ( $p > 0.05$ ;  $n = 16-18$ ; Mann-Whitney test). Symbols represent mean  $\pm$  S.E.M. B, Overall locomotor activity in an open-field was measured on day 2. GS967-treated mice showed a small, but significant increase in total distance traveled relative to untreated control mice, indicated by asterisk ( $p < 0.05$ ;  $n=13-16$ ; Student's t-test). C, On day 3 latency to fall from an accelerating rotarod showed no significant difference between GS967-treated and untreated control mice ( $p > 0.05$ ;  $n = 16-17$ ; Student's t-test).

**Supplemental Figure S2.** Seizure diary plot for *Scn8a*<sup>D/+</sup> mice undergoing continuous monitoring. Each line represents a single subject (1-7, Untreated; 9-15, GS967-treated). Black tick marks indicate a seizure event with a single tonic phase and orange tick marks represent seizure events with multiple tonic to tonic-clonic transitions. Recorded deaths are shown as triangles. Grey brackets indicate start and stop of continuous monitoring. Occasional brief monitoring gaps that account for <0.2% of total time (for husbandry or technical tasks) are omitted for presentation clarity. Seizure counts and calculated frequencies are summarized in Table 1.

**Supplemental Table S1.** Effects of GS967 on action potential (AP) parameters of WT and *Scn8a*<sup>D/+</sup> CA1 neurons

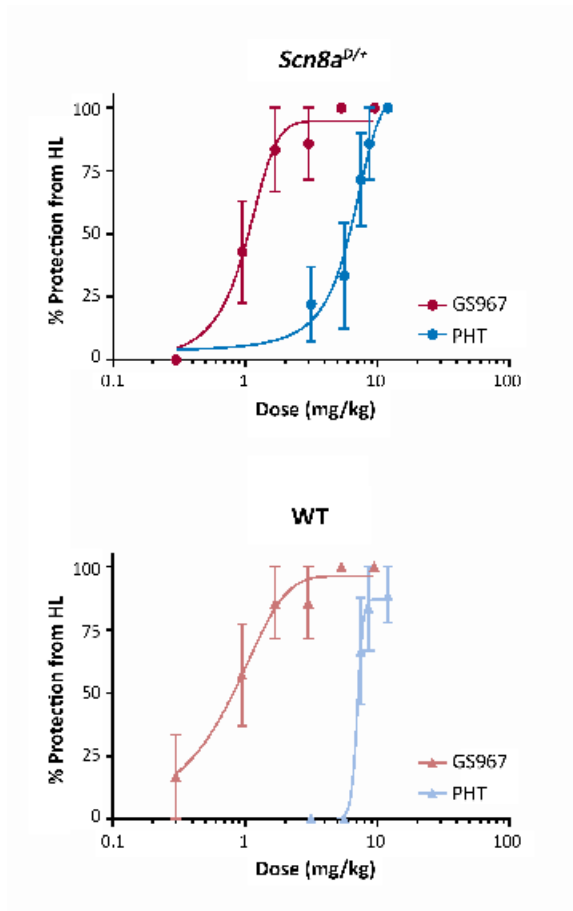


epi\_14196\_f1.tif



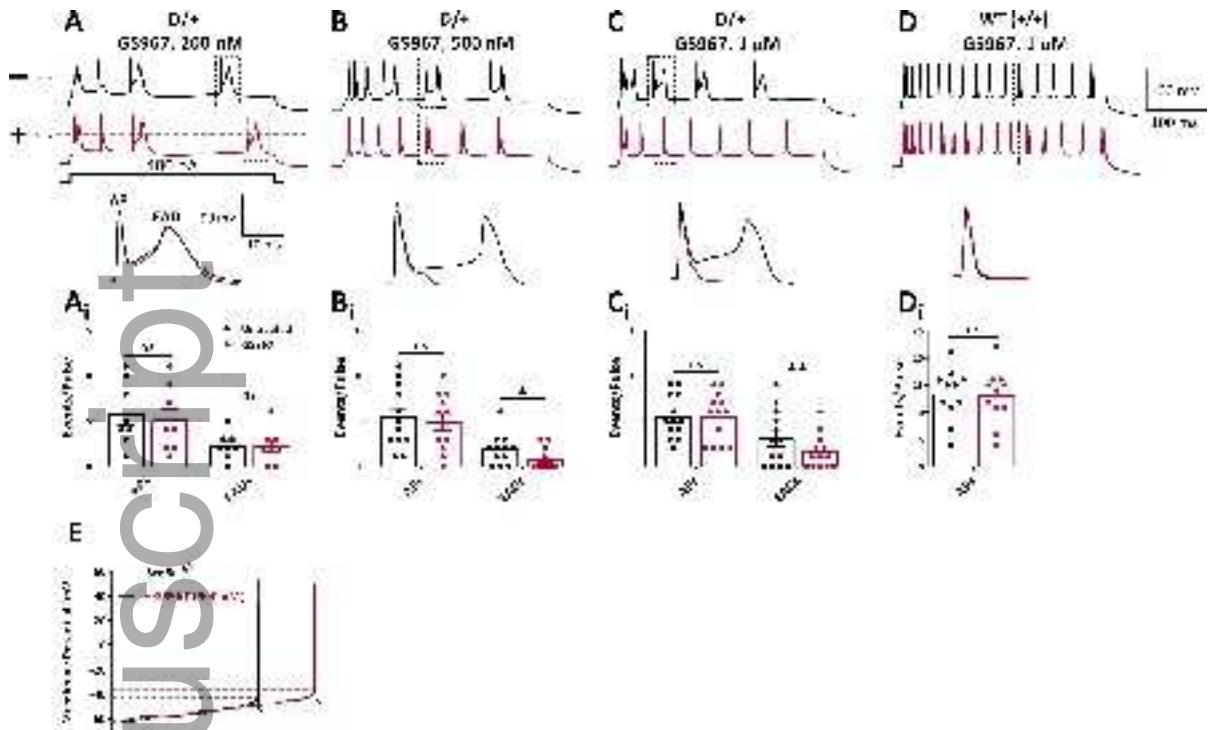
epi\_14196\_f2.tif

Author Manuscript

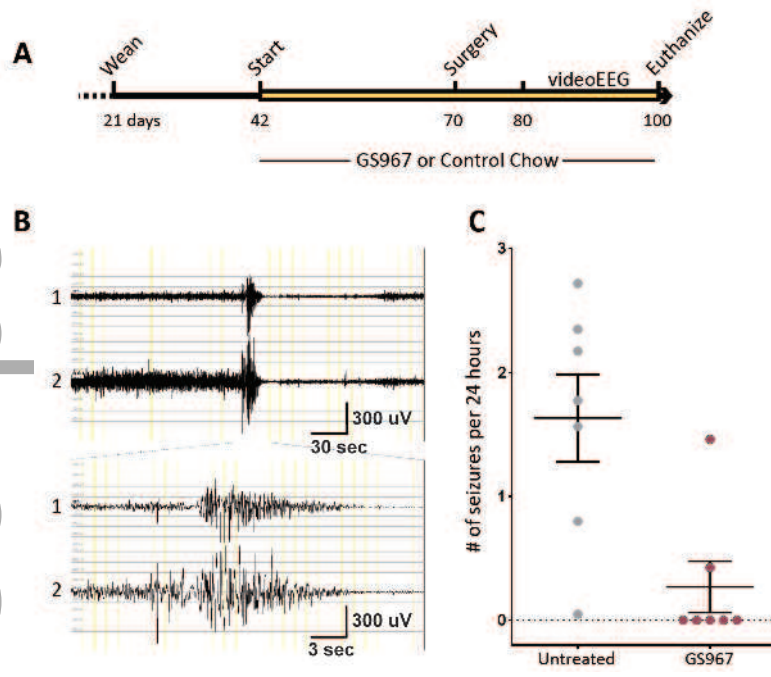


epi\_14196\_f3.tif





epi\_14196\_f4.tif



epi\_14196\_f5.tif